

# Synthesis and Characterization of Hydrophobic, Aprotically-Dispersible, Silver Nanoparticles in Winsor II Type Microemulsions

Abhijit Manna and B. D. Kulkarni\*

Chemical Engineering Division, National Chemical Laboratory, Pune-411 008, India

Krisanu Bandyopadhyay and K. Vijayamohan

Physical Chemistry Division, National Chemical Laboratory, Pune-411 008, India

Received May 20, 1997. Revised Manuscript Received October 7, 1997<sup>⊗</sup>

Dodacanethiol-capped silver “quantum dot” particles (Q-particles) have been synthesized using a novel biphasic microemulsion (Winsor II type) of diethyl ether/AOT/water. FT-IR investigations and elemental analyses support the encapsulation of silver particles by dodecanethiol while the transmission electron micrograph reveals an average size of 11 nm. The optical band corresponding to a surface plasmon of silver confirms the nanoparticle nature. The evidence from X-ray photoelectron spectroscopy investigation confirms the metallic state of silver ( $\text{Ag}^0$ ) and the encapsulation by thiol molecules. The thermogravimetric and differential thermal analysis indicates a heterogeneous interaction between thiol group and silver surfaces.

## Introduction

The possibility of a dramatic change in electronic properties by varying the size of metal and semiconductor particles has emerged recently as an area of important and fruitful research activity due to its fundamental and technological relevance. For example, synthesis of various particles of “quantum dots” with sizes varying from 1 to 100 nm have found promising applications in microelectronic devices,<sup>1</sup> photocatalysis,<sup>2</sup> electroluminescence and electrocatalysis,<sup>3</sup> reprography,<sup>4</sup> etc. When the electrons and holes are confined within the three-dimensional potential well, the continuum of states in the conduction and valence bands is broken down into discrete states with an energy spacing, relative to band edge, which is approximately inversely proportional to the square of the particle size.<sup>5,6</sup> They have a characteristic high surface-to-volume ratio, providing sites for the efficient adsorption of the reacting substrates leading to unusual size dependent chemical reactivity.<sup>7–9</sup>

Although synthesis of nanodimensional colloids in biphasic system was known earlier, the problems such as their stability and precise control of reactivity have been tackled only recently using different strategies. Size control is often sought either through the attachment of appropriate protecting agents, such as gelatins,

albumines, and other peptides, and macromolecules, such as polyethylene imine or polyvinylimidazole, on the surface of the cluster or to one another without leading to coalescence which results into the loss of their size-induced electronic properties. Another expedient method involves the use of self-assembled monolayer (SAM) formation with alkanethiols and amines for noble metal surfaces leading to the successful synthesis of stable “quantum dots.” For example, the work recently reported by Brust et al.<sup>10</sup> involves this type of a method using sodium borohydride reduction of an aqueous tetrachloroaurate in excess diethyl ether. Tetraoctylammonium bromide was used as a phase-transfer catalyst to exchange tetrachloroaurate ions from aqueous to organic phase. Although this is an efficient one-step method for the synthesis of nanoparticles, the transferable metal ion should be in the form of anionic complexes, and hence, this method cannot be extended to common water soluble salts of the metals such as simple salts of silver and copper.

The use of an inorganic phase in reverse micelles/microemulsions has received considerable attention for preparing semiconductor and metal particles including platinum group<sup>11,12</sup> and the noble metals.<sup>13–16</sup> Micelles/microemulsions are thermodynamically stable transparent liquid systems consisting of, at least, a ternary mixture of water, a surfactant, or a mixture of surface-active agents and oil. Depending on the proportion of

<sup>⊗</sup> Abstract published in *Advance ACS Abstracts*, November 15, 1997.

(1) Colvin, V. L.; Schlamp, M. C.; Alivisatos, A. P. *Nature* **1994**, *370*, 354.

(2) Hoffman, A. J.; Mills, G.; Yee, H.; Hoffmann, M. R. *J. Phys. Chem.* **1992**, *96*, 5546.

(3) Brus, L. *J. Phys. Chem.* **1986**, *90*, 2555.

(4) Hamilton, J. F.; Baetzold, R. C. *Science* **1979**, *205*, 1213.

(5) Chakarvorty, D.; Giri, A. K. In *Chemistry of Advanced Materials*; Rao C. N. R., Ed.; Blackwell Scientific Publication: Boca Roton, FL, 1993.

(6) Schmid, G. *Chem. Rev.* **1992**, *92*, 1709.

(7) Siegel, R. *Nanostruct. Mater.* **1993**, *3*, 1.

(8) Hirai, H.; Wakabayashi, H.; Komiyama, M. *Bull. Chem. Soc. Jpn.* **1986**, *59*, 367.

(9) Boakye, E.; Radovic, L. R.; Osseo-Asare, K. *J. Colloid Interface Sci.* **1994**, *163*, 120.

(10) Brust, M.; Walker, M.; Bethell, D.; Schiffrin, D. J.; Whyman, R. *J. Chem. Soc., Chem. Commun.* **1994**, 801.

(11) Chan, J. P.; Lee, K. M.; Sorensen, C. M.; Klabunde, K. J.; Hadjipanayis, G. C. *J. Appl. Phys.* **1994**, *75* (10), 5876.

(12) Boutonnet, M.; Kizling, J.; Stenius, P.; Maire, G. *Colloids Surf.* **1982**, *5*, 209.

(13) Fendler, J. H. *Chem. Rev.* **1987**, *87*, 877.

(14) Kurihara, K.; Kizling, J.; Stenius, P.; Fiedler, J. H. *J. Am. Chem. Soc.* **1983**, *105*, 2574.

(15) Petit, C.; Lixon, P.; Pileni, M. P. *J. Phys. Chem.* **1993**, *97*, 12974.

(16) Gan, L. M.; Chew, C. H. *Bull. Singapur Nat. Inst. Chem.* **1995**, *23*, 27.

suitable components and hydrophilic–lyophilic balance (HLB) value of the surfactant used, the formation of microdroplets can be in the form of oil-swollen micelles dispersed in water as for oil-in-water (o/w) microemulsion or water-swollen micelles dispersed in oil as for water-in-oil (w/o) microemulsion (reverse microemulsion). In the intermediate phase region between o/w and w/o microemulsions, there may exist bicontinuous microemulsions whose aqueous and oil domains are interconnected randomly in the form of sponge-like microstructures. In addition to single-phase microemulsions, several phase equilibria are known, namely Winsor systems.<sup>17</sup> A Winsor I (W I) system consists of an o/w microemulsion which is in equilibrium with an excess oil phase, while a Winsor II (W II) system is a w/o microemulsion which is in equilibrium with an excess aqueous phase. The Winsor III (W III) system is a bicontinuous microemulsion while a macroscopically single-phase microemulsion is denoted as a Winsor IV (W IV) system.<sup>11</sup> All of these systems maintain a certain microenvironment; the applications of W I and W II type systems in the synthesis of “quantum dot” particles is expected to avoid the limitations that may arise due to solubility constraints as mentioned earlier. It is known that the flexibility of the surfactant films, presence of additional stabilizing agents, and concentration of the reactants influence the final size of the product particles irrespective of the size of the microdroplets.<sup>17</sup>

We report here for the first time, the use of such an environment (Winsor II) for the synthesis of dodecanethiol-capped nanoparticles of silver. The microemulsion system consists of water/AOT/diethyl ether along with dodecanethiol, where dispersed microdroplets of water domains in organic bulk phase are in equilibrium with excess water. We prefer AOT as the surfactant due to its higher solubility in organic phase and its anionic polar headgroup which helps to extract metal cations from the aqueous to reverse micellar phase. The metal ions concentrated in the dynamic reverse microdroplets were reduced with sodium borohydride and consequently capped by dodecanethiol particles present in the system. The Q-particles were characterized by FT-IR, TEM, XPS, UV–vis, and TGA/DTA to reveal the nature of thiol-encapsulated, organically soluble, silver “quantum dots.”

### Experimental Section

The following chemicals were used: sodium borohydride and dodecanethiol (Aldrich, 98–99% purity), sodium bis-(2-ethylhexyl) sulfosuccinate, i.e., AOT (Sigma, 99%), silver nitrate (LOBA Chemie, 99.9%), and ethanol (BDH, 99.7–100%). Water was Milli-Q grade with a conductivity less than  $0.1 \mu\text{S cm}^{-1}$ .

Twenty milliliters of  $0.02 \text{ mol dm}^{-3}$  aqueous silver nitrate ( $\text{AgNO}_3$ ) solution and 80 mL of a  $0.04 \text{ mol dm}^{-3}$  AOT solution in diethyl ether were mixed together and stirred vigorously for 15 min. Subsequently it was allowed to separate into two distinct transparent phases for 5–10 min, resulting in a quantitative transfer of  $\text{Ag}^+$  ions from the aqueous to reverse microemulsion (diethyl ether) phase. To confirm such ion transfer, we kept one system for a long duration (48 h) under ambient conditions so that the color of the organic phase changes to blackish brown while very light coloration was

observed in the aqueous phase. Ninety milligrams ( $4.45 \times 10^{-4} \text{ mol}$ ) of dodecanethiol was then added to the rapidly stirring microemulsion for 5 min and allowed to stand. Next,  $0.2 \text{ mol dm}^{-3}$  of 20 mL freshly prepared  $\text{NaBH}_4$  aqueous solution was slowly added to the mixture with vigorous stirring; stirring was continued for 2 h to complete the reaction, and two phase separation was observed to follow. The deep brown reverse micellar phase containing a large quantity of precipitate was in equilibrium with a clear aqueous phase and this aqueous phase was separated. The solid waxy type powder product was extracted by filtration of diethyl ether solution through  $0.2 \mu\text{m}$  nylon filter paper under pressure. The precipitate was thoroughly washed with excess ethanol to eliminate AOT adsorbed on the surface of the particles. The so purified solid was dried completely at  $45^\circ\text{C}$  in vacuum. The product obtained was highly soluble in nonpolar organic solvents such as *n*-pentane, *n*-hexane, *n*-heptane, toluene but seems to be insoluble in polar solvents such as water, methanol, ethanol, propanol, and acetone.

FT-IR spectra were recorded on a Perkin-Elmer 16PC FT-IR instrument, using KBr pellet. The TEM analysis was performed with a transmission electron microscope (TEM unit Philips EM 301) for which the sample was prepared by evaporating a drop of dilute heptane solution of the particles onto an amorphous carbon-coated copper TEM grid. A Perkin-Elmer Lambda 3B double beam UV–vis spectrophotometer was used for the recording of UV–vis absorption of free thiol and particles in heptane. The X-ray photoelectron spectroscopy signals were recorded on a VG scientific ESCA 3MK II spectrometer operated at a base pressure better than  $10^{-9}$  Torr. The radiation source (Mg K $\alpha$ , 1253.6 eV) was used as a magnesium anode (Mg K $\alpha$ , 1253.6 eV) and a hemispherical mirror analyzer operated in the fixed retard ratio mode. Elemental analysis was conducted with a C, H, N, S, O elemental analyzer (Carlo Erba Instrument, Model EA 1108). The thermal stability of the nanoparticles were investigated by thermogravimetric and differential thermal analysis (TGA/DTA) (Sieco SII, SSC5100, instrument) at a heating rate of  $10^\circ\text{C}/\text{min}$  under nitrogen atmosphere.

### Results and Discussion

**Infrared Spectral Studies.** A comparison of the FT-IR spectra between 4000 and  $450 \text{ cm}^{-1}$  of dodecanethiol and encapsulated particles is shown in Figure 1 where all the important bands of the pure dodecanethiol at 3000–2840, 1200–800, 1350–1150, 1500–1150, 2600–2550, and  $700\text{--}600 \text{ cm}^{-1}$  are clearly seen.<sup>18</sup> The similarity of the features confirms (i) the presence of thiol as an essential component of the composite nanoparticles and (ii) that the thiol molecule is not leached out during several washing of the precipitate.

A close observation of above spectra (1a and 1b) reveals several interesting features. The band assigned to C–C stretching vibrations in the broad region of  $1200\text{--}800 \text{ cm}^{-1}$  is stronger compared to the free thiol probably due to an encapsulation effect, i.e., the intensity of the C–C stretching frequency is increased owing to the formation of an Ag–S bond. The C–H stretching and bending of the methyl group in the region  $3000\text{--}2040 \text{ cm}^{-1}$  seems to be invariant with respect to the capping. The distinct bands occurring at  $2956 \text{ cm}^{-1}$  due to asymmetric stretching ( $\nu_{\text{as}}\text{CH}_3$ ) and bands at  $2852 \text{ cm}^{-1}$  due to symmetric stretching ( $\nu_{\text{s}}\text{CH}_3$ ) also show a slight increase in intensity due to capping. The asymmetric stretching ( $\nu_{\text{as}}\text{CH}_2$ ) and symmetric stretching ( $\nu_{\text{s}}\text{CH}_2$ ) of the methylene groups occur near  $2925$  and  $2853 \text{ cm}^{-1}$ , respectively, and are superimposed on the previous bands.

(17) Lattes, A.; Rico, I.; de Savignac, A.; Samii, A. *Tetrahedron*, **1987**, *43*, 1725.

(18) Silverstein, R. M.; Bassler, G. C. *in Spectrometric Identification of organic compounds*, Wiley: & Sons, Inc.: New York, 1963.

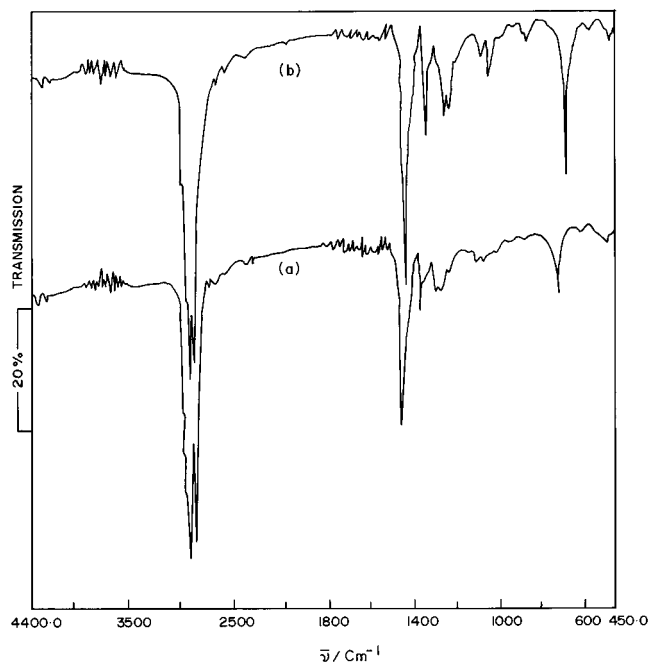


**Figure 1.** FT-IR spectra of (a) dodecanethiol and (b) nanoparticles synthesized in Winsor II type microemulsions at room temperature. KBr technique was used for recording of these spectra.

A more subtle change is observed over the 1550–600  $\text{cm}^{-1}$  range. The intensity of the symmetric bending vibration ( $\delta_s\text{CH}_3$ ) around 1375  $\text{cm}^{-1}$  along with the asymmetric bending vibration ( $\delta_{as}\text{CH}_3$ ) around 1465  $\text{cm}^{-1}$  of the methyl group are found to be increased to 15% and 9%, respectively, due to capping. The intensities of the bands resulting from methylene rocking vibration ( $\delta\text{CH}_2$ ) in which all of the methylene groups rock in phase appear at 720  $\text{cm}^{-1}$ , and the very weak bands for methylene twisting and wagging vibrations in the 1350–1150  $\text{cm}^{-1}$  region are dramatically increased as a result of capping. The precise reason for the enhancement of the intensities of all the maintained bands is not clear. A probable reason is the special orientation effects of the thiol molecule during the formation of self-assemblies on silver surfaces.

The S–H stretching band in the range of 2600–2550  $\text{cm}^{-1}$  is not observed in Figure 1a presumably due to its characteristic low intensity.<sup>18</sup> The specific stretching vibration assigned to the C–S linkage in the 700–600  $\text{cm}^{-1}$  region observed in both the cases (Figure 1a,b) shows no significant change on capping.

**Elemental Analyses.** Microanalysis of the thiol-capped cluster compounds for C, H, and S are 46.01, 8.01, and 11.51, respectively. The atomic percentage of C, H, S, are respectively as follows: 71.212, 12.948, and 15.840 were calculated, and 70.191, 12.250, and 17.559 were found. The fractional amount of C, H, and S, found in the elemental analyses are all in close agreement with the composition of the  $\text{C}_{12}$ -thiol, which supports the encapsulation. The ratio of the sum of the percentage of C, H, S (65.55%) and metallic content (assuming the rest is metal only) reveals that 3.5 silver atoms associate with 4 alkanethiol molecules. This ratio matches very closely with that obtained from TEM and TGA analyses.

**X-ray Photoelectron Spectroscopy.** The signals of the XPS spectra acknowledge the presence of Ag and

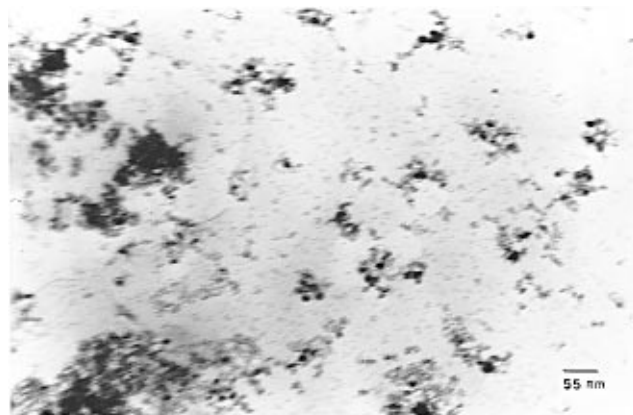


**Figure 2.** TEM of the dodecanethiol-encapsulated silver nanoparticles prepared in Winsor type II microemulsion. The micrographs were taken by evaporating a drop of dispersed solution of particles in heptane on carbon-coated TEM grid.

**Table 1. XPS Data for Sulfur and Silver Present in the Free Thiol and Silver Nanoparticles**

	sulfur ( $2p_{3/2}$ ), eV	silver ( $3d_{5/2}$ , $3d_{3/2}$ ), eV
free thiol, $\text{C}_{12}\text{H}_{26}\text{S}$	163.6	
metallic silver		367.9, 374.4
capped particles	162.6	368.4, 374.4

S in the synthesized composite particles. All the binding energies of corresponding elements (calculated on the basis of binding energy of carbon as 285 eV) are shown in Table 1. A high-resolution scan over the range 360–380 eV reveals a doublet of the Ag  $3d_{5/2}$  peak at 368.4 eV and the Ag  $3d_{3/2}$  peak at 374.4 eV, corresponding to a peak to peak separation of 6 eV due to the presence of the  $\text{Ag}^0$  state since the peak position, line shapes, and peak to peak distance of the silver doublet are standard measures of the silver oxidation state. The standard binding energies for the Ag doublet ( $3d_{5/2}$  and  $3d_{3/2}$ ) are 367.9 and 374.9 eV, i.e., the separation of the peaks is 7 eV.<sup>14</sup> The sulfur region exhibits a broad S 2p peak at 162.6 eV. This core level is shifted by nearly 1 eV to lower binding energy from the position expected for an undisturbed S–H bond in thiol. Moreover, the broad peak of the XPS signal suggests positive evidence for the heterogeneous bond formation with surface of the particles,<sup>19</sup> although the precise reason of this type of heterogeneous bond formation is not clear. The absence of peak at nearly 532 eV indicates formation of neither silver oxide ( $\text{AgO}$ ,  $\text{Ag}_2\text{O}$ ) nor adsorbed oxygen on the surface.

**Transmission Electron Microscopy.** The transmission electron micrograph (bright field image) of the particles is depicted in Figure 2. The image shows that all the particles are almost spherical and are within 5–17 nm size range. The TEM micrograph also shows that the particles taking part in the nanostructure formation maintain their distinct character and do not agglomerate into large clusters. The short distance between particles in large aggregates may be due to the interaction of the nonpolar part of the thiol molecules. The histogram corresponding to electron micrograph in Figure 3 shows that more than 60% of the particles possess a diameter of 11 nm. A calculation based on

(19) Laibinis, P. E.; Whitesides, G. M.; Allara, D. L.; Tao, Y.; Parikh, A. N.; Nuzzo, R. G. *J. Am. Chem. Soc.* **1991**, *113*, 7152.

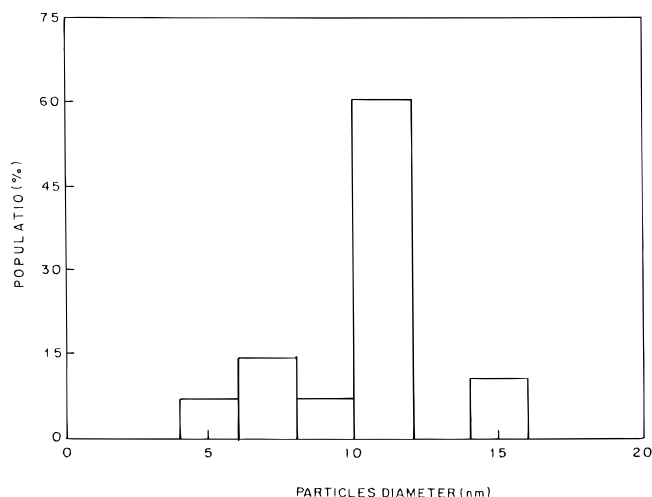


**Figure 3.** Histogram corresponding to the electron micrograph given in Figure 2.

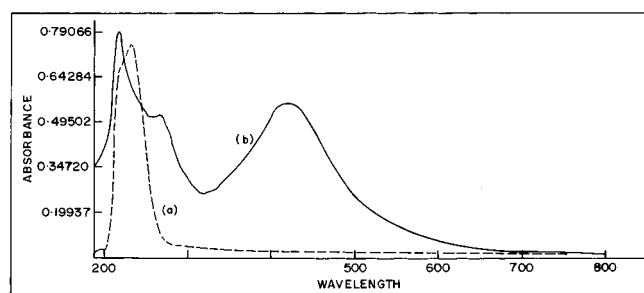


**Figure 4.** UV-vis spectra of (a) free thiol and (b) nanocomposite particles in *n*-heptane.

the average particle size (11 nm) reveals that each of the three silver atoms at the surface of the particle interacts with four thiol molecules, in excellent agreement with the results of the elemental analysis.<sup>20</sup>

**Ultraviolet-Visible Spectroscopy.** A comparison of optical absorption spectra of the capping agent alone and the capped metal clusters is shown in Figure 4. The electronic energy levels and optical transition in "roughened" silver have been extensively studied and the 4d to 5sp interband transition generally occurs around an energy corresponding to 320 nm (i.e., 3.8 eV).<sup>21a,b</sup> For thiol-capped silver nanoparticles, the characteristic plasmon absorption band around 425 nm is expected to be invariant with respect to the size of the particles. The red shift of the absorption spectra supports the formation of Q-dot particles.<sup>21a</sup> The broadening of the spectra arises due to the smaller particles size than the mean free path of the electrons (>52 nm for silver). A rough estimation of the particles size on the basis of available optical absorption for silver clusters indicates an average size of around 14 nm.<sup>21c</sup> This is in excellent agreement with the results on the basis of transmission electron micrograph's results.

**Thermogravimetric and Differential Thermal Analysis.** Figure 5 shows the thermogravimetric and differential thermal analysis of the silver nanoparticles. Apart from the initial slow change in weight, the TG curve exhibits a sharp weight loss in the range 270–

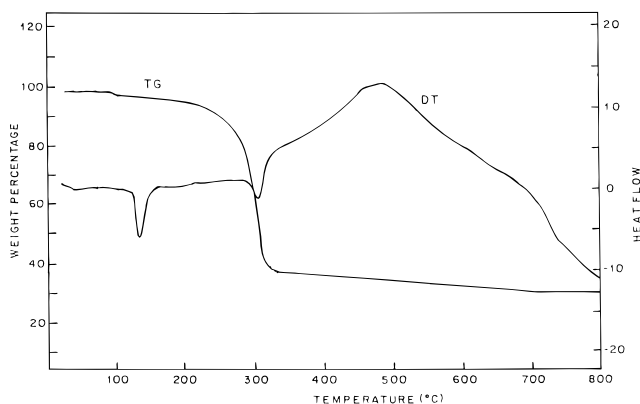


**Figure 5.** TGA/DTA for dodecanethiol-capped silver "quantum dot" synthesized in Winsor II type microemulsion of diethyl ether/AOT/water system.

320 °C. Since the boiling point of dodecanethiol is in the range 266–283 °C, the above weight loss can be possible due to the loss of thiol molecules.<sup>22</sup> The extension of stability of capped molecules (decomposition temperature ~320 °C) further confirms the Ag<sup>0</sup>-S bond formation during the preparation stage. Further evidence for this comes from the observed higher rate of weight loss covering a large temperature range (~50 °C). The total weight loss of the particles in the above temperature range is 63.41%, and there is very little change up to 800 °C, probably due to the formation of metallic silver. The above results could be further illustrated by the DTA profile; first, an endothermic peak is observed at 135 °C, probably owing to the reorganization of the chains of thiol molecules on the surface of the Ag cluster. The endothermic peak at 300 °C supports the desorption of thiol molecules by the breaking of Ag<sup>0</sup>-S bonds. The additional broad exothermic curve (covering a large range) may be due to the larger decomposition range of thiol molecules.

The stability studies have shown that the compound is very stable both in solution and powder forms under ambient conditions. This was confirmed by UV-vis and TGA/DTA characterization after storage for 8 months, suggesting the absence of aging effects such as coalescence or flocculation. However, after 8 months the TGA/DTA analysis shows very small change (~1 wt %) attributed to volatile materials.

## Conclusion

The synthesis and characterization of stable alkanethiol-capped nanoparticles of an average size of 11 nm, using novel Winsor II type microemulsion for the first time, demonstrate the dual role of the AOT in the formation of microemulsion and extraction of oppositely charged metal ions from aqueous to organic phase. These particles form a stable dispersion in nonpolar solvents in ambient conditions. The FT-IR, microanalysis, and XPS results confirm that the deep-brown waxy powder product is a dodecanethiol-encapsulated metallic silver cluster. Further the transmission electron micrograph and UV-vis spectroscopy confirm the size of the clusters in "quantum dot" range. These type of particles are promising for several applications, including the manufacturing of high-density integrated cir-

(20) Leff, D. V.; Ohara, P. C.; Heath, J. R.; Gelbart, W. M. *J. Phys. Chem.* **1995**, *99*, 7036.

(21) (a) Kreibitz, U. *J. Phys. F: Metal Phys.* **1974**, *4*, 999. (b) Beaglehole, D. and Hunderi, O. *Phys. Rev. B*, **1970**, *2*, 309. (c) Hengelin, A. *J. Phys. Chem.* **1993**, *97*, 5457.

(22) Terrill, R. H.; et al. *J. Am. Chem. Soc.* **1995**, *117*, 12537.

cuits, information storage devices, optical detector, and high-quality color copiers.<sup>23–26</sup>

**Acknowledgment.** The authors wish to thank to Mr. A. Sinha and Mr. Parag Thanki for recording FT-

IR spectra, Dr. A. B. Mandale for taking XPS spectra, Mr Sukhen Haite for taking UV–vis spectra, and Dr. S. S. Ramdasi for microanalysis. Financial support (for A.M.) from the Council of Scientific and Industrial Research (CSIR), New Delhi, India, and (for K.B.) University Grants Commission (UGC), New Delhi, India, are gratefully acknowledged.

CM9703740

---

(23) Fendler, J. H. *Chem. Mater.* **1996**, *8*, 1616.

(24) Cohen, M. L.; Knight, W. D. *Physics Today* **1990**, *43*, 42.

(25) Service, R. F. *Science* **1996**, *271*, 920.

(26) Reetz M. T.; Winter, M. *J. Am. Chem. Soc.* **1997**, *119*, 4539.